

**Error Analysis for a Long-Range Lightning Monitoring Network of Ground-  
Based Receivers in Europe**

Themis G. Chronis and Emmanouil N. Anagnostou

Department of Civil and Environmental Engineering

University of Connecticut

Storrs, CT 06269

Submitted to *Journal of Geophysical Research-Atmospheres*

February 2003

Corresponding author: Dr. Emmanouil N. Anagnostou, Civil and Environmental Engineering,  
University of Connecticut, Storrs, CT 06269, 860-486-6806 (voice), [manos@engr.uconn.edu](mailto:manos@engr.uconn.edu).

### **Abstract**

An experimental long-range lightning detection system consisting of a network of six ground-based radio receivers has been deployed in Europe and has been operating since June 2001. The receivers measure the electromagnetic signal emitted by a lightning source at the Very Low Frequency, between 5 and 15 KHz (sferics), which can propagate over thousands of kilometers in the earth-ionosphere wave-guide. In this study, lightning retrievals from the experimental network are compared against more definitive lightning measurements from other sources to investigate issues on long-range lightning location retrieval accuracy and detection efficiency. The study concentrates over three regions: U.S. East Coast/Northwestern Atlantic, Africa continent, and within the network (Spain), using information provided by the U.S. National Lightning Detection Network, the Lightning Imaging Sensor aboard the Tropical Rainfall Measurement Mission satellite, and the Spanish National Lightning Network, accordingly. The nature of the errors involved in the lightning location retrieval is quantified, and a new approach for improving the retrieval via modeling of the sferics wave propagation velocity is proposed. The location retrieval error is shown to vary between 40 and 400 km (with a mode at 220 km) for very long ranges, while within the network it does not exceed the 40 km (with a mode at 20 km). The error reduction from modeling the sferics velocity is about 12%, which corresponds to about 20 km at long-range retrievals. It is also shown that the location retrieval error has a strong directionality. The long-range detection efficiency varies from 15% to 75% (with a mode of about 35%), and does not seem to depend on the time of day. Error statistics derived from the above simulation for this experimental network agreed well with the statistics retrieved from independent measurements in all three regions.

## 1. Introduction

Lightning detection has been a subject for research since late 1940s. The first lightning studies were launched mainly to investigate the propagation of electromagnetic waves excited by lightning strokes (Schumann, 1954). Today, lightning research is focused primarily on continuous monitoring of precipitation from thunderstorms (Greco et al., 1999; Goodman, 1990), ozone/NO<sub>x</sub> atmospheric concentration (Chameides, 1986), aviation safety, short-term weather forecasting (Alexander et al., 1999) and global climate studies (Williams, 1992). With the development of technology to monitor lightning over large regions (continents and beyond) based on ground based Very Low Frequency (VLF) radio receivers (Lee, 1986a,b), lightning information can now be used to extend the capabilities of high-resolution rainfall estimation from satellite observations (Morales and Anagnostou, 2002). This will have significant implication on global water cycle research because precipitation is one of the most important components of the hydrologic cycle and is needed for monitoring the climatic state of water.

An experimental long-range lightning detection system (Zeus) based on a network of six ground based VLF radio (the so called atmospherics or the contraction: sferics) receivers has been installed and operated by the National Observatory of Athens-Greece on the European continent. The system was developed by Resolution Displays, Inc., and is designed to use the latest computing technology, signal processing algorithms, geographic positioning systems and communications networking to improve the state-of-the-art in receiver design at long-range frequencies (system description is provided at <http://sifnos.engr.uconn.edu>). The radio receivers are situated in six remote locations around Europe, selected for their low manmade electric noise interferences. These locations are near Birmingham (UK), Roskilde (Denmark), Iasi (Romania),

Larnaka (Cyprus), Mt. Etna (Italy), and Evora (Portugal). The deployment of Zeus receivers was completed in June 15, 2001. Since then lightning has been monitored over Europe and surrounding waters, as well as the U.S. East/Coast North Atlantic, West Asia and Central Africa with decreased detection efficiency (Anagnostou et al., 2002).

Each Zeus receiver measures the vertical electric field as a time series by including a time stamp synchronized by a Global Positioning System (GPS) clock, which represents the sferics waveform. The Arrival Time Differences (ATD) between the sferics waveforms from all possible pairs of receivers (15 pairs for the existing 6 receivers) is extracted by maximizing the temporal cross-correlation of the two time series. The intersection between those ATD's defines a lightning fix, namely, location and time of the lightning source that originated the sferics waves. This is an inverse problem that requires a sferics wave propagation (speed and earth path) model to simulate the array of ATD's for an assumed lightning source location on earth and an optimization scheme for determining the lightning fix associated with a minimum least square difference of modeled versus observed ATD's (Lee, 1986a). According to Volland (1995) the Arrival Time Difference method, compared to other radio direction finding techniques, has the advantage that eliminates polarization effects from the propagating signal. The Zeus system is designed to primarily measure cloud-to-ground (CG) lightning, as its bandwidth is in the range of 7 to 15 kHz where CG return strokes have a spectrum energy peak as opposed to a cloud-to-cloud (CC) which has its peak at around 30 kHz (Grandt, 1992). Research based on a similar system operated in Northern Atlantic and the U.S. East Coast for a three month period has shown that the system can detect about 80% of the CG lightning events occurring within the network periphery, while less than 15% of the CC lightning (Morales, 2001).

This paper investigates the nature of the errors involved, based on Zeus system, with respect to lightning location at medium to long ranges (hundreds to thousands of kilometers) as well as certain ways of ameliorating their magnitude. Furthermore, a stochastic error model is developed based on ATD error statistics derived from simulations and independent measurements (from reference sources over the U.S. East Coast, Africa and Europe). Finally, we examine the system's long-range CG lightning detection efficiency through comparison with an efficient ground based network in the U.S. East Coast. The paper is structured as follows: in the next section we describe the locating algorithm, while in Section 3 we describe the model used for simulating the sferics propagation (traveling path, velocity etc.). In Section 4 we present the algorithm's error statistics through comparisons with reference lightning observations and present a modeling framework for determining the systems location error over the globe. In Section 5 we discuss the system's long-range lightning detection efficiency.

## 2. Locating Algorithm – The Inverse Problem

According to Lee (1986b), each ATD from a pair of receivers yields a parabolic locus of points on the earth's surface (ATD parabolas). As an example, an ATD pair between stations “*i*” and “*j*” would be defined as:

$$ATD^{i-to-j} = \frac{S_i}{V_i} - \frac{S_j}{V_j} \quad (1)$$

where  $S_i$  and  $S_j$  are the distances (km) from the lightning source to the  $i^{\text{th}}$  and  $j^{\text{th}}$  receiver, while  $V_i$  and  $V_j$  are the associated wave propagation velocities (km/sec). As discussed in the

Introduction, determining the location of the lightning source where the measured sferics waves originated from is an inverse problem solved by finding a point in space that minimizes the following cost function:

$$\chi^2 = \sum_{i=1}^{15} \left\{ \frac{1}{\sigma_i^2} \left( ATD_i^{Measured} - ATD_i^{Simulated}(V, u) \right)^2 \right\} \quad (2)$$

where the “measured” and “simulated” superscripts symbolize ATD’s measured from Zeus receivers and simulated from Equation (1) for an assumed location on Earth ( $u$ ) and sferics wave velocity ( $V$ ). The  $\sigma^2$  is the variance of the combined measurement and modeling error for each ATD pair, while subscript “i” is the ATD pair index (15 ATD). A fundamental assumption made in formulating Equation (2) is that ATD modeling/measurement errors are unbiased and uncorrelated. The geometrical equivalent of the cost function minimum is the cross section location of more than three ATD parabolas (Lee, 1986a).

As discussed by Koshak (2001), retrieving the location of a lightning stroke on the basis of time differences is highly dependent on the lightning’s relative location to the network. We further explore this issue through simulation by considering two distinct lightning locations (one inside the network and the other outside), and determine the  $\chi^2$  maps associated with assumed locations around the globe. The ATD’s were simulated based on a sferics wave propagation model discussed in a later section. Figure 1 shows the  $\chi^2$  maps for the two hypothetical locations and two different network configurations. As mentioned above, a lightning location is retrieved by determining the minimum value in the  $\chi^2$  map, which as shown in Figure 1 is affected by the network’s sensor geometry. Note that multiple minima in (2) are possible so that the solution in

general is not unique. A non-unique solution (often related to a local minimum) is called the “parallel baseline effect” (Lee, 1986b). The two upper panels of Figure 1 present the Zeus network under its present receiver configuration, while left and right panels show  $\chi^2$  maps for a hypothetical lightning over Europe and the Atlantic Ocean, respectively. The lower panels present alternate network geometry for the same hypothetical lightning stroke locations as in the upper panels. It is apparent that for a lightning location two different network geometries can give distinctly different regions of  $\chi^2$  minima. Cases with small regions of  $\chi^2$  minima (such as upper left and lower right panels) are associated with the most accurate lightning retrievals. Cases with large extends of  $\chi^2$  minima region can be associated with significant errors in lightning retrieval. These errors can be magnified even further by noise introduced in the system from various sources; some of the most important are anomalous electromagnetic signal propagation, weak time stamp correlation, clock synchronization errors. In a subsequent section, issues like error introduced from inaccuracies in modeling the sferics signal velocity will be discussed.

### **3. Modeling the lightning induced sferics wave propagation**

The wave excited by a cloud to ground (CG) lightning stroke is simulated by an electromagnetic wave excited by a vertical Hertzian dipole source between a spherical earth and a concentric homogeneous isotropic atmosphere (Bremmer, 1949). This wave propagates through an imperfect (finite conductivity) and curved wave-guide (earth-ionosphere wave-guide) while it suffers from a transition between mediums; that is from air to a non-perfectly conducting medium (e.g. dry areas with a typical conductivity value of  $10^{-4}$  S/m), or bounce off a varying

conductance ionosphere (Volland 1995). The approach taken in this study is based on the VLF propagation theory proposed by Al’pert and Fligel (1957) and Wait (1961, 1970). The goal is to retrieve the propagation velocity of the wave inside the earth ionosphere wave-guide. The solution is achieved by solving equations (3) through (8) shown below, for the unknown parameter C. Solution techniques may involve (since the equations are nonlinear with respect to C) some iterative techniques (e.g. Newton)

$$\frac{2}{3}ka(C^2 + 2\frac{h}{a})^{\frac{1}{2}} + ia(C^2 + \frac{2h}{a}) + i \log \left[ \frac{w'_2(t) - qw_2(t)}{w'_1(t) - qw_1(t)} \right] - (4\pi - 1)\frac{\pi}{2} = 0 \quad (3)$$

$$w_1(t) = e^{-i\pi/3} \left(\frac{-\pi t}{3}\right) H_{1/3}^{(2)} \left[ \frac{2}{3}(-t)^{3/2} \right] \quad (4)$$

$$w_2(t) = e^{+i\pi/3} \left(\frac{-\pi t}{3}\right) H_{1/3}^{(2)} \left[ \frac{2}{3}(-t)^{3/2} \right] \quad (5)$$

$$w'_1(t) = e^{-i\pi/3} \left(\frac{-\pi t}{3}\right) (-t) H_{1/3}^{(2)} \left[ \frac{2}{3}(-t)^{3/2} \right] \quad (6)$$

$$w'_2(t) = e^{+i\pi/3} \left(\frac{-\pi t}{3}\right) (-t) H_{1/3}^{(1)} \left[ \frac{2}{3}(-t)^{3/2} \right] \quad (7)$$

$$t = -\sqrt{(ka/2)^{\frac{1}{3}} C} \quad (8)$$

where  $\text{Real}\{C\} = c/v$ , the ratio of the phase velocity of light in vacuum  $c$  to the actual velocity of propagation ( $v$ ).  $H^{(2)}$ ,  $H^{(1)}$  are Hankel functions of second and first order accordingly,  $h$  (Km) is the ionosphere D layer height, which is the main boundary that affects VLF propagation,  $a$  (Km) is earth’s radius,  $k$  the wave number and  $q$  is the reflectivity index of the associated boundaries. For further discussion on the above equations the interested reader is referred to Wait (1970).

The applicability of the aforementioned method lies on the fact that a typical CG return stroke has a spectrum peak at about 10.1 KHz, a wavelength of about 30 Km that is comparable to the “width” of the earth-ionosphere wave guide where the wave is traveling. Along the geographical path from lightning source to receiver, the major parameters that affect the signal propagation velocity are: hour of the day, day of year and electrical conductivity of upper and lower boundaries of the wave-guide (D-layer ionosphere height and earth surface accordingly). Values for the ionospheric conditions are calculated using the International Reference Ionosphere (IRI 95) model. Regarding the electrical ground conductivities, the World Atlas Of Electrical Ground Conductivities (1993) has been used.

Figure 2 shows examples of the velocities retrieved by solving equations (3) through (8) for a sferics wave traveling over different surface media (water/soil) as well as for different spectrum peak frequencies. The results shown in Figure 2 are in close agreement with velocity plots shown in Chapman et al. (1966). To accommodate variations in the phase velocity along the sferics wave paths to the different receivers, the simulated ATD’s of equation (1) are now represented by breaking the equation in discrete paths as follows:

$$ATD^{i-to-j} = \left[ \frac{S^i_1}{V^i_1} + \frac{S^i_2}{V^i_2} + \dots + \frac{S^i_n}{V^i_n} \right] - \left[ \frac{S^j_1}{V^j_1} + \frac{S^j_2}{V^j_2} + \dots + \frac{S^j_n}{V^j_n} \right] \quad (9)$$

where S and V symbolize the path ground distances and associated signal velocities. The number of discrete paths is determined as the ratio of the source-to-sensor distance to path resolution (in this study is selected to be 100 km). For each discrete path the velocity is determined through equations (3-8) based on the path’s average ground electric conductivity properties and ionosphere height determined from IRI95 model for that geographical location

and time/date. The above calculations are pre-computed and assigned in Equation (9) through a look-up table based on discrete categories of geographic locations, time of day, day of month and month in a year.

#### **4. Error analysis of lightning location retrieval**

##### *a. Experimental analysis*

Three independent lightning detection sources are selected for validating Zeus lightning recordings. The first source is the U.S. National Lightning Detection Network (NLDN) that provides CG lightning measurements at high temporal (1-2  $\mu\text{sec}$ ) detail. NLDN consists of about 105 stations recording time, polarity, signal strength and number of strokes of each CG lightning flash occurring within the United States and surrounding waters. A combination of time-of-arrival and direction finding technique is used to locate a flash from NLDN measurements. Depending on the location within the network, the system's locating accuracy is normally within 500 meters, with a detection efficiency of 80% to 90% of the total CG flashes (Orville et al 1994). We use NLDN data over a limited region spanning within (85W, 25N) and (70W, 55N), where its locating accuracy and detection efficiency is high. For other regions over the globe (e.g. African continent and the Atlantic Ocean) we used limited measurements from the Lightning Imaging Sensor (LIS) aboard the orbiting Tropical Rainfall Measuring Mission (TRMM) satellite. LIS is monitoring individual storms within a field-of-view (FOV) of 80 seconds, which is long enough to estimate the lightning flash rate. Location of lightning flashes is determined to within 5 km over a 600 x 600  $\text{km}^2$  FOV (Christian et al.1989; Goodman et al.

1993). Although providing global coverage within a  $\pm 40^\circ$  latitude zone, their sampling frequency is limited to about one overpass per day for a fixed site on Earth. For assessment of Zeus lightning retrievals within the European periphery we used measurements from the Spanish Lightning National Network (SLNN), a system similar to the NLDN. The area window used for validation purposes was between (10W, 35N) and (10E, 42N).

The Zeus retrieval error from a matched ground (or space) reference lightning source is defined in terms of direction ( $\varepsilon_d$ ) and distance ( $\varepsilon_l$ ), where the  $\varepsilon_l$  is computed using the earth spherical oblate model while direction error is evaluated as,

$$\varepsilon_d = \arctan \left\{ \left| \frac{\lambda^{Valid} - \lambda^{Zeus}}{\phi^{Valid} - \phi^{Zeus}} \right| \right\} \quad (10)$$

where  $(\lambda, \phi)$  are the latitudinal and longitudinal values (in degrees) of any given point on earth. An issue in determining the location error experimentally based on a reference lightning measurement is the selection of an appropriate space and time window inside which two strokes are considered belonging to the same event. As shown in previous studies the spatial window selection can affect the error distance statistics, in particular the tails of the error distribution (Morales, 2001). We chose to bind the spatial solution domain to a distance where two independent sources (in this case NLDN and LIS) give consistent error statistics for the same area domain, which in this case is the aforementioned window (85W, 25N) to (70W, 55N) over the U.S. East Coast. This distance was determined to be around 3.5 degrees, which is similar to the distance used in Morales (2001) and Boccippio et al. (2000). This space window was applied to the other regions where we used LIS and SLNN reference data. The time window selected

was similar to past studies (Christian et al., 1992; Boccippio et al., 2000; Koshak et al., 2000; Morales, 2001), namely, we used 2  $\mu$  sec for comparisons with the NLDN and SLNN data, and 500 milliseconds for matching with LIS group-product lightning locations (LIS/OTD Software Guide, 1998). Overall, 12,000 matches were found between Zeus and NLDN, 3,000 between Zeus and LIS and finally 1,200 for Zeus and SLNN.

Figures 3 through 5 show the cumulative histograms of the two error parameters ( $\epsilon_l$  and  $\epsilon_d$ ) for the two long-range regions (U.S. East Coast and Central Africa) and within the network (Spain). Several observations are made from these plots. First, that the error statistics determined based on LIS and NLDN reference data over the same region are very similar and consistent in terms of both distance and directional error. A second observation from the same group of figures is that the error distances fall in the same range of values for the two long-range regions (Africa and U.S. East Coast), while the directional error differs significantly between these two regions. The main error angles vary between  $45^\circ$  and  $60^\circ$  (approximately North-East or South-West directions) for the Northern Atlantic and U.S. east coast region, while over the African continent the angles vary from  $70^\circ$  to  $100^\circ$  (approximately North or South directions). Simulations will demonstrate that this directional tendency is not random but largely associated with the relative location of a lightning stroke and network geometry. A last observation is that the distance error within Europe is significantly lower than what we find at long ranges, varying from 5 km to a maximum of 40 km with a mode at around 20 km. The directional error statistics (not shown here) within the network did not show any directional dominance of the location error. Below we describe a simulation framework designed to explain the location error statistics determined in this section.

*b. Simulation of location error*

We used the physically based sferics wave propagation model to simulate theoretical ATD's for the lightning source locations of the reference data associated with matched Zeus-reference source pairs in U.S. East Coast (NLDN), Central Africa (LIS), and Spain (SLNN) regions. The simulated ATD's ( $ATD_{\text{simulated}}$ ) were compared to the corresponding measured ATD's ( $ATD_{\text{measured}}$ ) to determine the Zeus ATD measurement error as follows:

$$\varepsilon_{ATD}^i = ATD^i_{\text{Measured}} - ATD^i_{\text{Simulated}} \quad (11)$$

The ATD measurement error is assumed to be normally distributed and uncorrelated for the various ATD pairs. The mean  $\overline{\varepsilon_i}$  and variance  $\sigma_i^2$  of the ATD error were determined from the matched Zeus-reference (NLDN, LIS and SLNN) lightning retrieval pairs. The ATD measurement error presented above represents a number of error sources including wave propagation effects, noise in determining the ATD values from Zeus waveforms, and GPS clock errors, among others. In Table 1 we present the error variances for the different ATD's determined from the three regions (U.S. East Coast, African continent, and Spain). The error variances are in the range of 15 to 20  $\mu\text{sec}$  for the Spain region, while slightly higher (20-50  $\mu\text{sec}$ ) for the U.S. East Coast/Northern Atlantic and the African continent. This increase is realistic given the added error sources due to the longer signal propagation and its interaction with a varied surface background (of varying electrical conductivity). In the African region the variances are slightly higher, which is due to propagation errors further amplified by the Sahara desert (extremely dry conditions). In a similar work, Grandt (1990) found relevant results,

regarding the signal propagation from Africa. The computation of the error correlation matrix for the various ATD's presents cross-correlation statistics mostly below 0.5, which supports our assumption of uncorrelated ATD errors.

The determined ATD error statistics are used in a Monte Carlo simulation framework to quantify their effect on Zeus lightning location retrieval over the globe. The simulation framework consists of the following steps:

- (1) Define discrete locations of hypothetical lightning sources;
- (2) Simulate the theoretical ATD's based on the wave propagation model;
- (3) Generate a large number (10,000) of errors for each ATD based on the error statistics presented above;
- (4) Generate equal number of Zeus's ATD measurement arrays by corrupting the theoretical ATD's with the randomly generated ATD errors;
- (5) Retrieve the lightning location from each generated Zeus's ATD measurement array based on the locating algorithm described in Section 2;
- (6) Determine the distance ( $\epsilon_l$ ) and directional ( $\epsilon_d$ ) errors for all retrievals using the defined lightning source location as reference.

From the Monte Carlo simulation results we derive cumulative frequencies of the location error parameters ( $\epsilon_l$  and  $\epsilon_d$ ) for the three validation regions considered in the previous section. The cumulative frequencies are shown in Figures 3 through 5 (broken lines). It is apparent that there is close agreement between the measured and simulated error statistics for both distance and directional errors in all three regions.

The simulation framework is devised to evaluate the system's location error statistics over an area ranging from 0N and 90W to 55N and 55E for a canonical grid of 10-degree pixel

resolution. The simulated Zeus retrieval locations from each realization in the simulation framework are plotted on Figure 6 (left panel). The strong directionality and magnitude of location error over certain regions on Earth is apparent. The further the lightning source is located from the network the greater the probability is that the error will be magnified by the parallel baseline effect. For a visual comparison with observations, Figure 6 (right panel) shows Zeus lightning retrievals recorded during a day (05/06/2002) over the same region (the selected validation regions are highlighted with rectangles). It is worth noting that the “long-tailed” sferics shown in the Zeus data coincide with the non-unique  $\chi^2$  areas as highlighted in Figure 1, and the “long-tailed” sferics retrievals simulated by the Monte Carlo simulation exercise. The presented error statistics and simulation framework will be used to investigate scenarios of new sensor(s) configuration for an extension of the existing network in the African continent and beyond. In the following section we investigate the significance of using the described physically based model for the sferic wave propagation versus a simplified single velocity approximation for long-range lightning location retrieval accuracy.

#### *d. Significance of sferic wave modeling*

In the previous section we quantified the statistics of error embedded in the lightning location retrieval. As mentioned before, the lightning induced sferics wave does not have a fixed propagating velocity; consequently, a locating algorithm has to efficiently include the velocity variation of the propagating signal in the inverse solution (Lee, 1990). In this section we investigate the significance in terms of location error of the proposed modeling approach versus a retrieval based on a fixed signal velocity. For this purpose the 12,000 NLDN and Zeus

matched cases were used to determine cumulative frequencies of the location error between NLDN and Zeus retrieved locations retrieved using path varying and fixed signal velocities. The cumulative error frequencies are plotted in Figure 7. It is showing that modeling the sferics wave velocity reduces the location retrieval error by about 12% consistently for almost all error quantiles. This translates to a decrease in location error of about 20 km at long ranges and below 1 km within the network.

## **5. Long range detection efficiency**

An important aspect of any lightning monitoring system is defining its detection efficiency. This is particularly important for long-range detection where attenuation can bring the signal below the noise floor of the sensor. According to Chapman and Macario (1956), Taylor (1960a and b) and Challinor (1967) the 10.1 kHz portion of the VLF spectrum attenuates at an approximate rate of 2 to 5 dB/Mm for both daytime and nighttime conditions depending mostly on ground reflectivity-conductivity index, the ionosphere (D-layer) height, as well as the direction of the propagation (Taylor and Lange, 1958). We selected an area of approximately  $10^5 \text{ Km}^2$  over the U.S. East Coast where both NLDN and Zeus recordings exist to evaluate the detection efficiency of our system at long range. The NLDN network was exclusively used due to its similarity with the sferics network (namely they both detect mostly CG flashes) while LIS and the Spanish network do not distinguish between CG and intra-cloud (CC) flashes. The detection efficiency was determined using the following approach:

- 1) Cold cloud clusters (brightness temperature below 255 K) were delineated based on GOES Infrared (IR) measurements; the recorded U.S. NLDN lightning strokes within the cluster were counted for a time window of  $\pm 15$  minutes around the IR measurement time.
- 2) For each NLDN lightning location in a cluster, a matched Zeus fix is searched within a 2  $\mu$  sec and  $3.5^\circ$  time and space window and if identified is considered a matching pair.
- 3) For the number of NLDN lightning strokes ( $N_{NLDN}$ ) in a cluster, the number of matched Zeus and NLDN ( $N_{NLDN|ZEUS}$ ) pairs are counted and the detection efficiency is defined as:

$$r(\%) = 100x \frac{N_{NLDN|ZEUS}}{N_{NLDN}}$$

Figure 8 shows cumulative histograms of the detection efficiency values ( $r$ ) determined based on  $\sim 1,200$  cloud clusters during day and nighttime. The detection efficiency is shown to have a mode at around 40% and values ranging from 5% to 95%. It is also shown that the DE is practically unaffected by the time of day. This is expected given that sferics signals primarily traveled over water (Atlantic Ocean) to reach the receivers so consequently over a medium that favors (at least compared to dry soil) propagation. What would really affect the Zeus's detection efficiency is the noise base floor of the receivers and parameters directly related to the quality of the signal (power released during the lightning stroke etc.) or the noise in the signal (e.g., due to a low conductivity medium). Those factors are difficult to quantify and apply to a theoretical model of detection efficiency.

## 6. Conclusions

Lightning is a meteorological parameter that can be measured continuously at the global scale on a real time basis. This study targets some critical issues regarding the long-range (thousands of kilometers) lightning detection. The limitations as well as the interferences between the emanating errors introduced during the location retrieval of a lightning event were investigated. We have shown that the detection can be an ill-posed inverse problem for certain combinations of network configuration and source location. Depending on the location of the lightning source, the measurement noise (either propagation or sensor-related) can be magnified according to the geometry of the network giving an inverse solution with non-distinctive  $\chi^2$  minima. Altering the network geometry is a way to eliminate this type of error, according to the area coverage needs. This kind of error analysis can be performed by doing computer simulations. For this purpose theoretical location error results were compared against experimental error analysis derived through ground and space based reference lightning measurements over three regions on earth (U.S. East Coast/North-West Atlantic, African continent, and Spain).

The analysis showed close agreement between experimental and simulation-based results in terms of distance and directionality error statistics. The distance error varied between 40 and 400 km (with a mode at 220 km) for very long ranges, while within the network it does not exceed 40 km (with a mode at 20 km). The directionality error is around  $45^\circ$  in the Northern Atlantic/U.S. East Coast, and about  $90^\circ$  over the African continent, while within the network there is no distinct directionality of the location error. The long-range detection efficiency varies from 15% to 75% (with a mode at  $\sim 35\%$ ), and it does not seem to depend on the time of day. In

2003, Zeus will be expanding in the African region with five additional sensors to be deployed in Ethiopia, Tanzania, South Africa, Nigeria, and Senegal. Future work on location accuracy and long range detection efficiency will continue on the basis of comparing the recordings from Zeus network in Africa using the African network as validation and vice versa. Validation exercise can be used in direct combination with LIS datasets, in order to achieve a higher confidence level of accuracy, especially over the African continent.

*Acknowledgements:* This study was supported by a *NASA New Investigator Program* award under Grant NAG5-8636. The first author was supported by a NASA Earth System Science Graduate Student Fellowship. The experimental lightning network in Europe was funded by the Greek General Secretariat for Research and Development, Ministry for Development, through a ‘Center of Excellence’ grant to the National Observatory of Athens.

## 7. References

- Alexander, D.G, Weinman J.A, Karyampudi V. Mohan, Oslon, W.S, Lee, A.C, The effect of assimilating rain rates derived from satellites and lightning on forecasts of the 1993 superstorm, *Journal Of Climate*, pp 1433-1448, 1999.
- Anagnostou, E.N., Chronis, T., and Lalas, D., New Receiver Network Advances Long-Range Lightning Monitoring, *EOS Feature Article*, 83, 555&559, 2002.
- Al'pert, Ya. L. and Fligel, S.D., Propagation of ELF and VLF waves near the earth, *Consultants Bureau, New York-London*, 1957.
- Boccippio, D.J., Driscoll, K., Hall, J., Buechler, D., LIS/OTD Software Guide, *Global Hydrology and Climate Center*, 1998.
- Boccippio, D.J., and Coauthors, The Optical Transient Detector (OTD): Instrument characteristics and cross sensor validation, *J. Atmos. Ocean. Tech.*, 17, 441-458, 2000.
- Bremmer, H., Terrestrial Radio waves, *Elsevier Press, New York*, 1949.
- Challinor, R.A., The phase velocity and attenuation of audio-frequency electromagnetic waves from simultaneous observations of atmospheric at two spaced stations, *J. Atmos. Terr. Phys.*, 299, 803-810, 1967.
- Chameides, W.L., The role of lightning in the chemistry of the atmosphere, in The Earth's electrical Environment, *National Academy Press, Washington, D.C.*, 70, 1986.
- Chapman, F.W. and Macario, R.C.V., Propagation of audio frequency radio waves at great distances, *Nature*, 177, 930, 1956.
- Christian, H.J. Blakeslee, R.J., and Goodman, S.J., The detection of lightning from geostationary orbit. *J. Geophys. Res.*, 94, 13,329-13,337, 1989.

- Christian, H.J. Blakeslee, R.J., and Goodman, S.J., Lightning Imaging Sensor (LIS) for the Earth Observing System, *NASA Technical Memorandum 4350, MSFC, Huntsville, AL.*, 1992.
- Goodman, S.J., Predicting thunderstorm evolution using ground based lightning detection networks, *NASA Tech. Memo*, TM-10352, 210 pp., 1990.
- Goodman, S.J., and Christian, H.J., Global observations of lightning. Atlas of Satellite Observations Related to Global Change, Edited by R. Gurney, J. Foster, and C. Parkinson. Cambridge University Press, New York, 191-219, 1993.
- Grandt, Christopher, Thunderstorm Monitoring in South Africa and Europe by means of Very Low Frequency Sferics, *J. Geophys. Res.*, Vol. 97, NO. D16, Pages 18, 215-18,226, November 20, 1992.
- Koshak, W. J., Solakiewicz, R. J., TOA Lightning Location Retrieval on Spherical and Oblate Spheroidal Earth Geometries, *J. Atmos. and Ocean. Tech.*, 18, 187-199, 2001.
- Koshak, W.J., Blakeslee, R.J., and Bailey, J.C., Data retrieval algorithms for validating the Optical Transient Detector and the Lightning Imaging Sensor, *J. Atmos. Ocean. Tech.*, 17, 279-297, 2000.
- Lee, A.C.L., An experimental study of the remote location of lightning flashes using a VLF arrival time difference technique, *Quart.J.R. Met. Soc.*, 112, 203-229, 1986a.
- Lee, A.C.L., An operational system for remote location of lightning flashes using a VLF arrival time difference technique, *J. Atmos. and Ocean. Tech.*, 3, 630-642, 1986b.
- Lee, A.C.L., Bias elimination and scatter in lightning location by the VLF arrival time difference technique, *J. Atmos. and Ocean. Tech.*, 6, 43-49, 1990.
- Greco M., Anagnostou, E.N., and Adler, R.F., Assessment of the Use of Lightning in Satellite Infrared Rainfall Estimation, *Journal of Hydrometeorology*, pp 211-221, 2000.

- Morales, C., and Anagnostou, E.N., Extending the Capabilities of High-Frequency Rainfall Estimation from Geostationary-Based Satellite Infrared via a Network of Long-Range Lightning Observations, *Journal of Hydrometeorology*, 2003 (in press).
- Morales, C., Continuous Thunderstorm Monitoring: Retrieval of Precipitation Parameters from Lightning Observations, *Ph.D. Thesis*, Department of Civil and Environmental Engineering, University of Connecticut, Storrs, CT 06269, pp 231, 2001.
- Orville, R.E., Cloud-to-Ground Lightning Flash Characteristics in the Contiguous United States: 1989-1991, *J. Geophys. Res.*, Vol. 5., 10833-10841, 1994.
- Schumann, W.O., and Koning, H., Uber die Beobachtung von Atmospheric bei geringsten Frequenzen, *Naturwiss-senschaften*, 41, 183, 1954.
- Taylor, W.L., Daytime attenuation rates in the vlf band using atmospheric, *J. Res. Nat Bur. Stand.*, 64D (Radio Prop.), 349, 1960a.
- Taylor, W.L., VLF, attenuation rates for east to west and west tot east daytime propagation using atmospheric, *J. Geophys. Res.*, 65, 1933, 1960b.
- Taylor, W.L., and Lange, L.J., Some characteristics of vlf propagation using atmospheric waveforms, *Proc. Second Conference on Atmos. Electricity*, p.609, Pergamon Press, London, 1958.
- Volland H., Handbook of Atmospheric Electrodynamics, Vol. 2, 1995.
- Wait, J.R., A diffraction theory for L.F sky wave propagation, *Journal Geophys. Res.*, Res., 66, num. 6, 1713-1724, 1961.
- Wait, J.R, Electromagnetic waves in stratified media, Pergamon Press, 1970.
- Williams, Earle R., The Schumann resonance: a global tropical thermometer, *Science*, 256, 1184, 1992.

Williams, Earle R., Global Circuit Response to Seasonal Variations in Global Surface Air Temperature, *Monthly Weather Review*: Vol. 122, No. 8, pp. 1917–1929, 1994.

World Atlas of Ground Conductivities, *International Telecommunications Union*, R-91-1, 1993.

Table 1. Standard deviations of the ATD measurement errors (in  $\mu\text{sec}$ ) determined based on reference lightning data from three different regions.

<b>U.S.</b>	<b>Africa</b>	<b>Europe</b>
26.7	69.1	15.3
24.7	40.9	20.4
27.6	67.1	17.5
42.8	33.6	13.6
54.25	24.5	17.0
14.57	55.2	23.5
34.4	71.3	15.8
51.7	56.5	21.1
66.6	78.7	20.7
23.7	72.9	12.6
40.5	68.0	23.6
56.5	75.2	19.8
21.1	45.7	15.6
39.9	80.6	13.7
21.6	50.0	21.4

## Figure Captions

Figure 1: Contours representing the  $\chi^2$  values described in (2) for different network configurations, where crosses represent a hypothetical lightning stroke location and solid squares show the network's receiver locations. White color pinpoints the region of minimum  $\chi^2$ .

Figure 2: Propagation velocity for a spherical wave traveling over water (dotted)/soil (solid) surface media for different spectrum peak frequencies. The ionosphere height of the D-layer is at 86 km.

Figure 3: Cumulative frequency of distance (left panels) and directional (right panels) error determined over the U.S. East Coast/North West Atlantic Ocean using as reference NLDN (thick-solid line) and LIS (dotted line) data. The panels also show cumulative histograms of error determined through simulation over the same region (solid thin line).

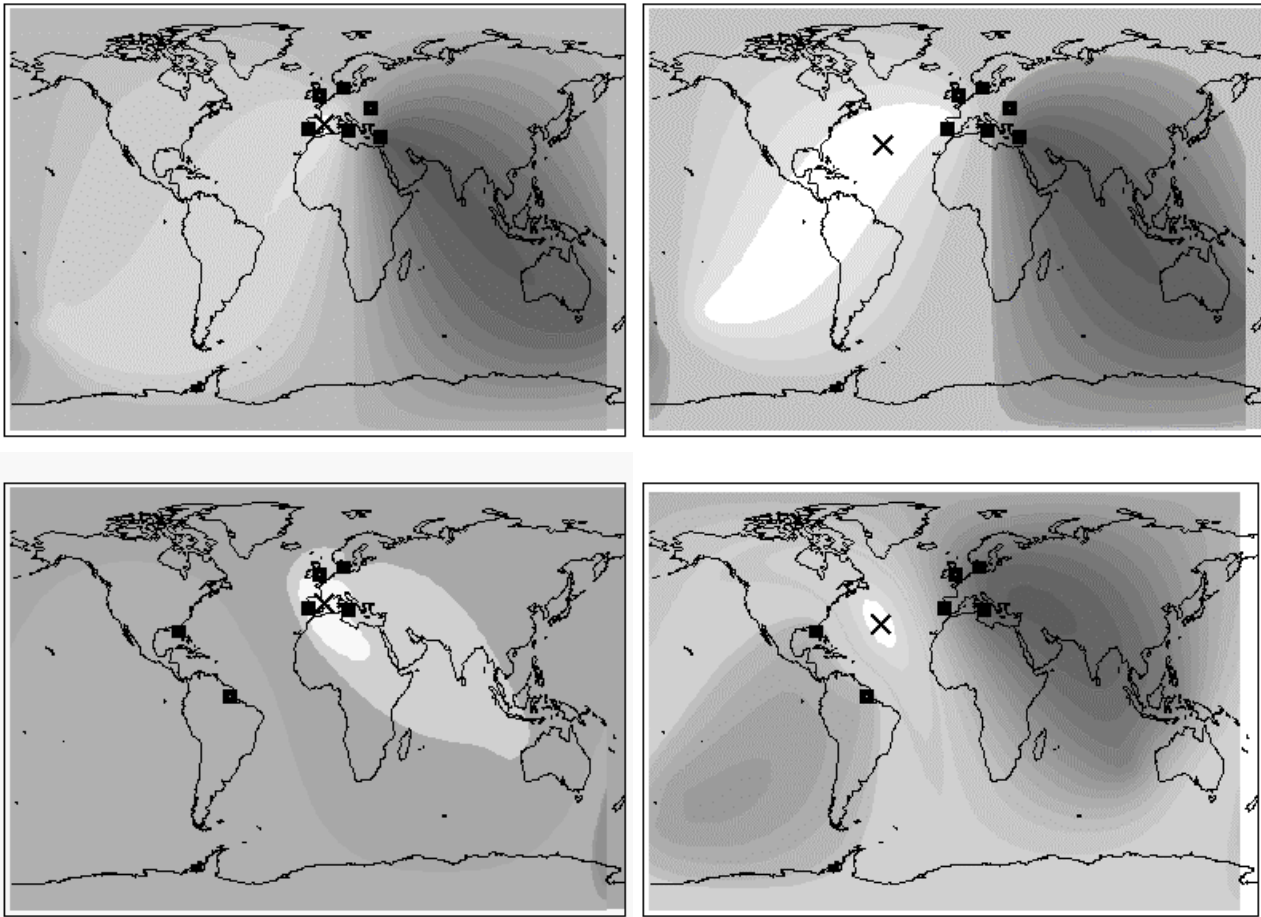
Figure 4: Cumulative frequency of distance (left panels) and directional (right panels) error determined over the African continent using as reference LIS (dotted line) data. The panels also show cumulative histograms of error determined through simulation over the same region (solid thin line).

Figure 5: Cumulative frequency of distance error determined over the Europe-Spain area using as reference the SLNN data (dotted line). The panels also show the corresponding cumulative histogram of distance error determined through simulation over the same region (solid thin line).

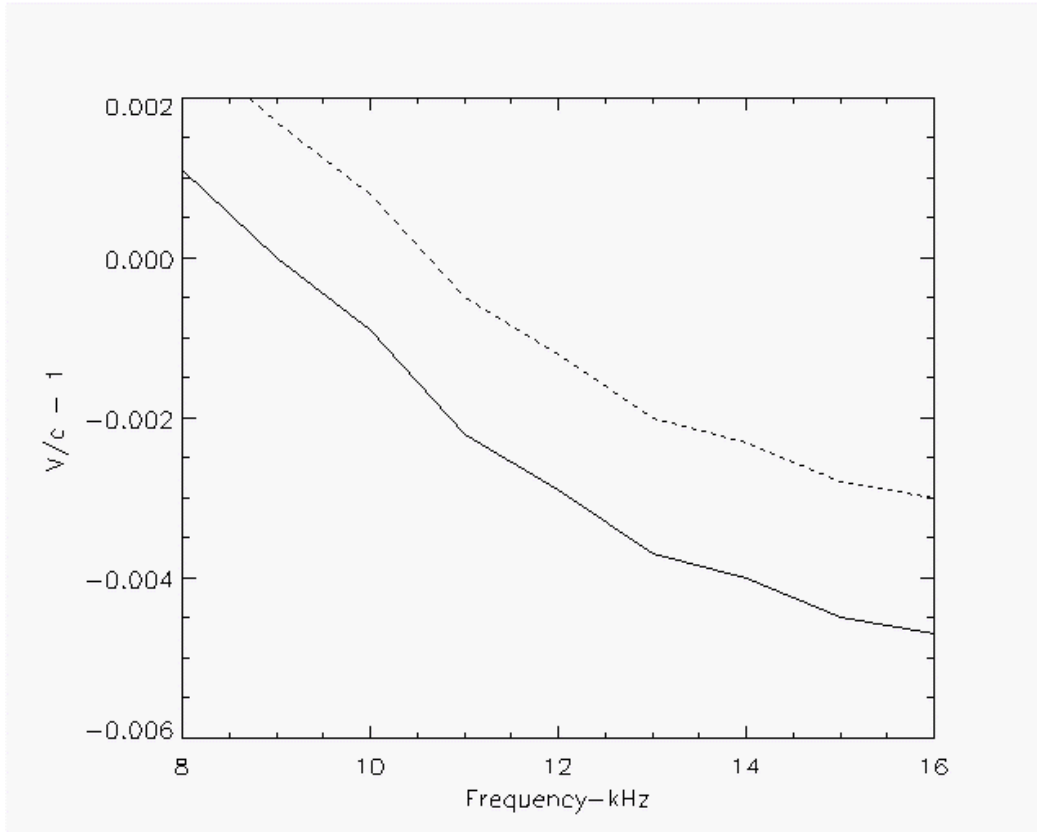
Figure 6: Left panel shows the scatter plot of retrieved locations determined through simulation. The right figure shows an example of lightning locations retrieved by Zeus network in one day (05/06/02). The rectangular regions show the areas where assessment of the simulation framework has been performed.

Figure 7: Cumulative frequencies of location retrieval errors determined over the U.S. East Coast based on a modeled sferics wave velocity versus a fixed (speed of light) velocity assumption.

Figure 8: Cumulative frequency of Zeus's detection efficiency over the U.S. East Coast area for day (solid) and night (dotted) cases.



**Figure 1:** Contours representing the  $\chi^2$  values described in (2) for different network configurations, where crosses represent a hypothetical lightning stroke location and solid squares show the network's receiver locations. White color pinpoints the region of minimum  $\chi^2$ .



**Figure 2:** Propagation velocity for a sferics wave traveling over water (dotted) and soil (solid) surface media for different spectrum peak frequencies. The ionosphere height of the D-layer is at 86 km.

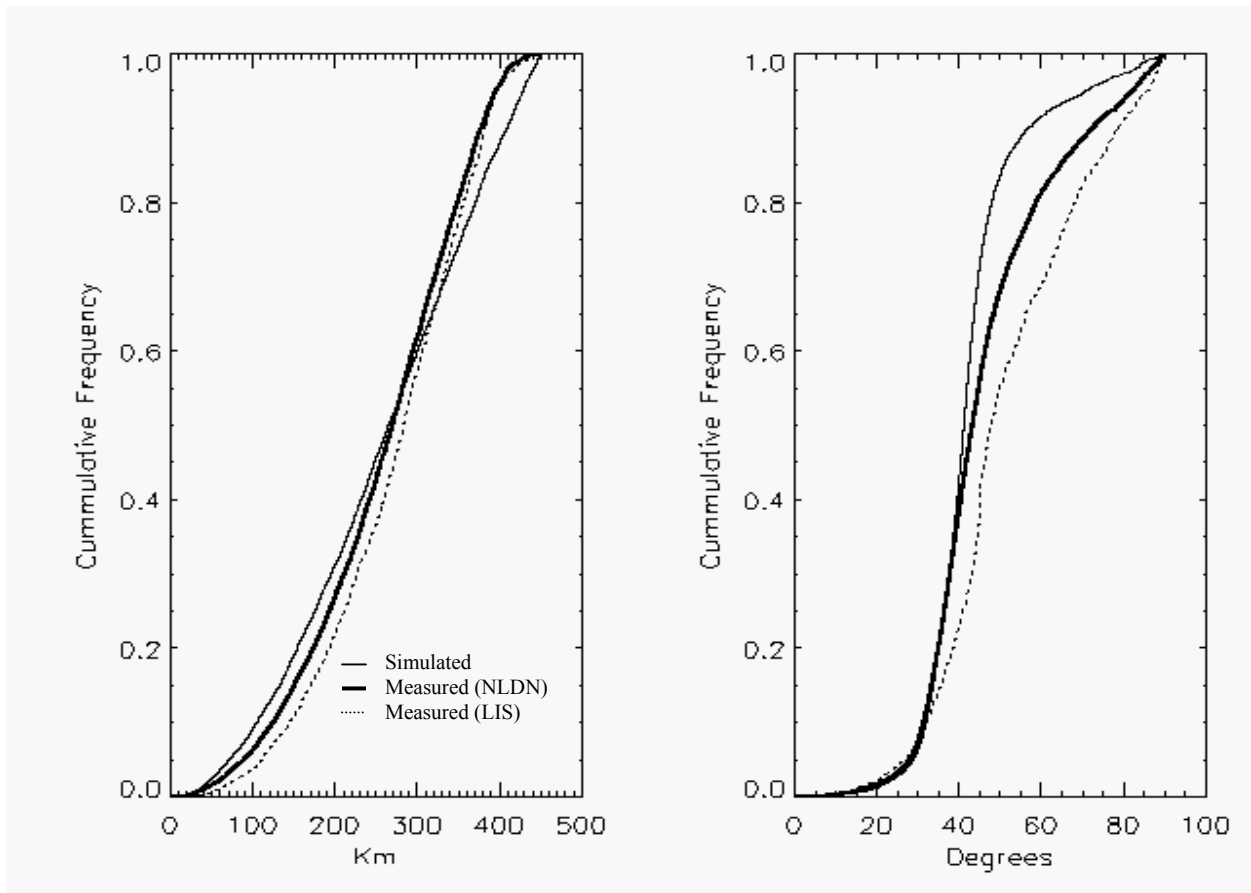


**Figure 3:** Cumulative frequency of distance (left panels) and directional (right panels) error determined over the U.S. East Coast/North West Atlantic Ocean using as reference NLDN (thick-solid line) and LIS (dotted line) data. The panels also show cumulative histograms of error determined through simulation over the same region (solid thin line).

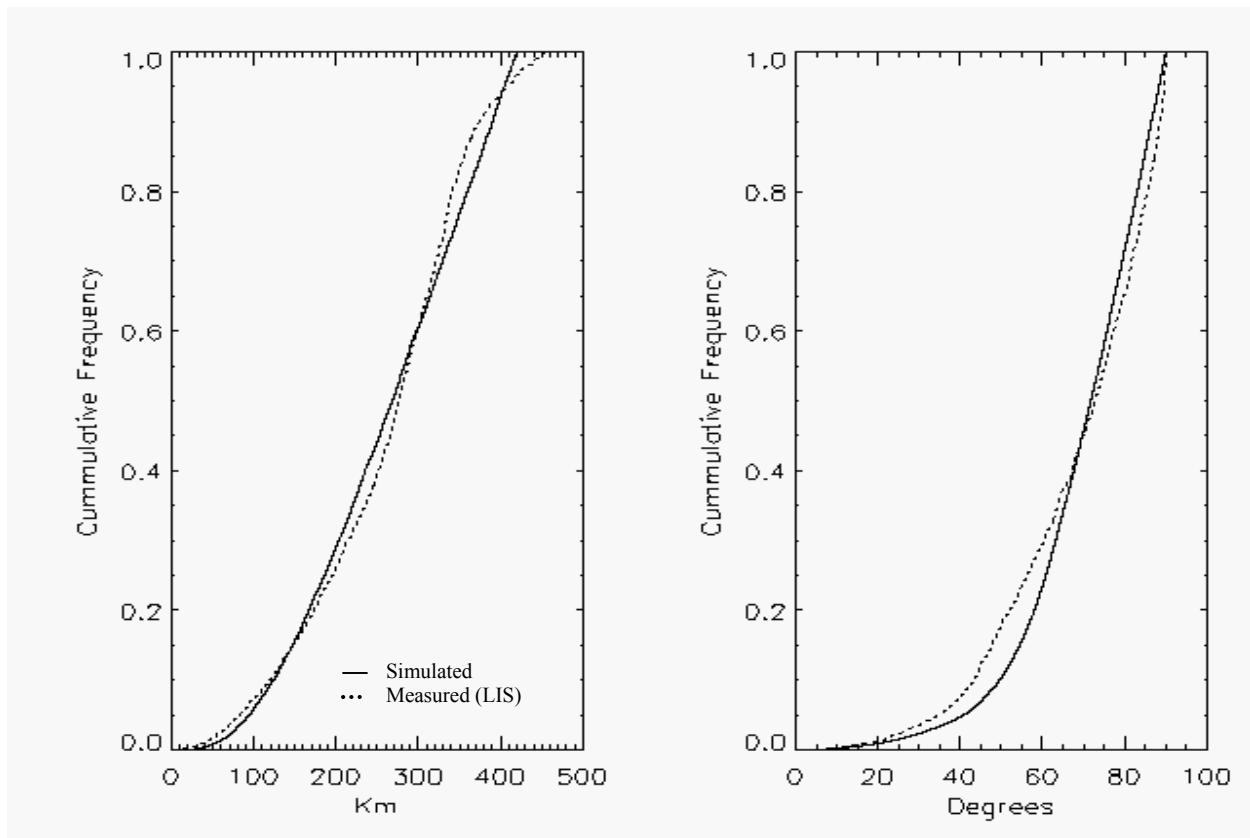


**Figure 4:** Cumulative frequency of distance (left panels) and directional (right panels) error determined over the African continent using as reference LIS (dotted line) data. The panels also show cumulative histograms of error determined through simulation over the same region (solid thin line).

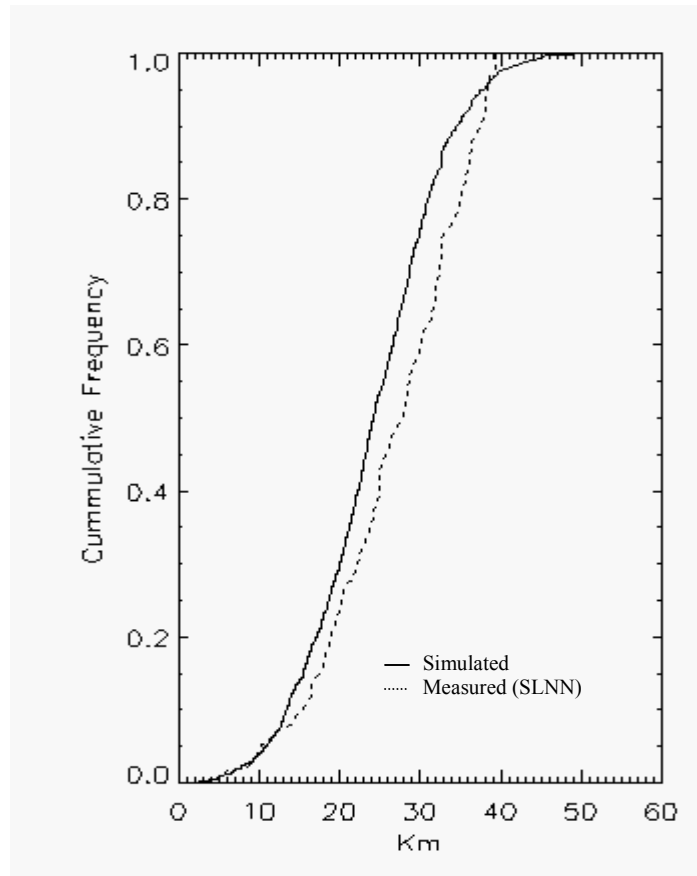


**Figure 5:** Cumulative frequency of distance error determined over the Europe-Spain area using as reference the SLNN data (dotted line). The panels also show the corresponding cumulative histogram of distance error determined through simulation over the same region (solid thin line).

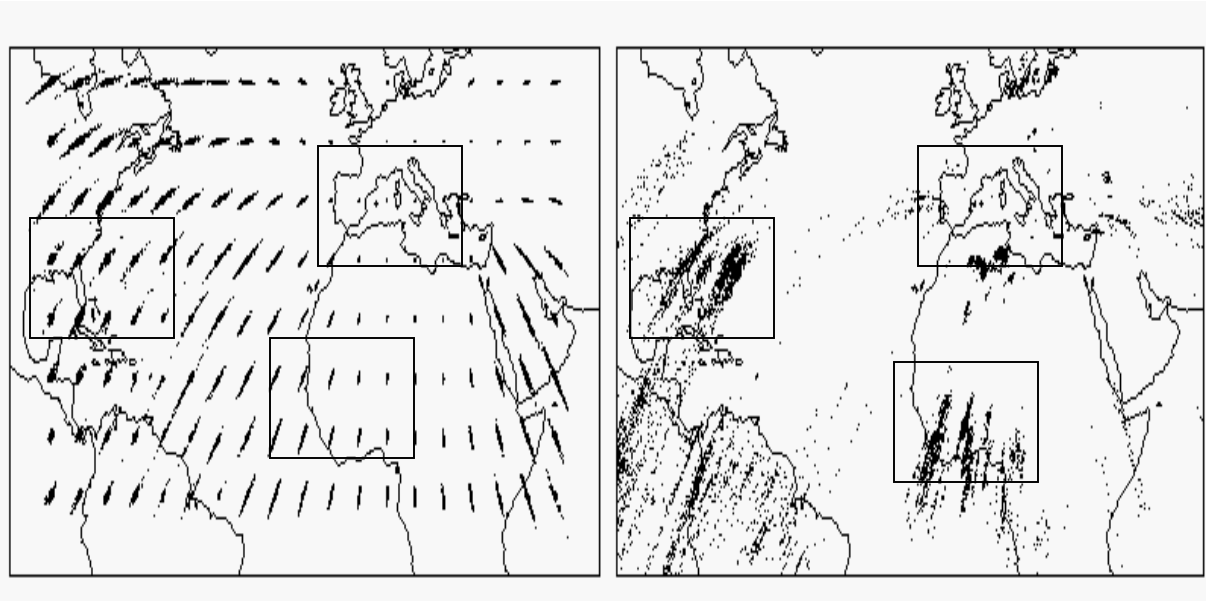


**Figure 6:** Left panel shows the scatter plot of retrieved locations determined through simulation. The right figure shows an example of lightning locations retrieved by Zeus network in one day (05/06/02). The rectangular regions show the areas where assessment of the simulation framework has been performed.

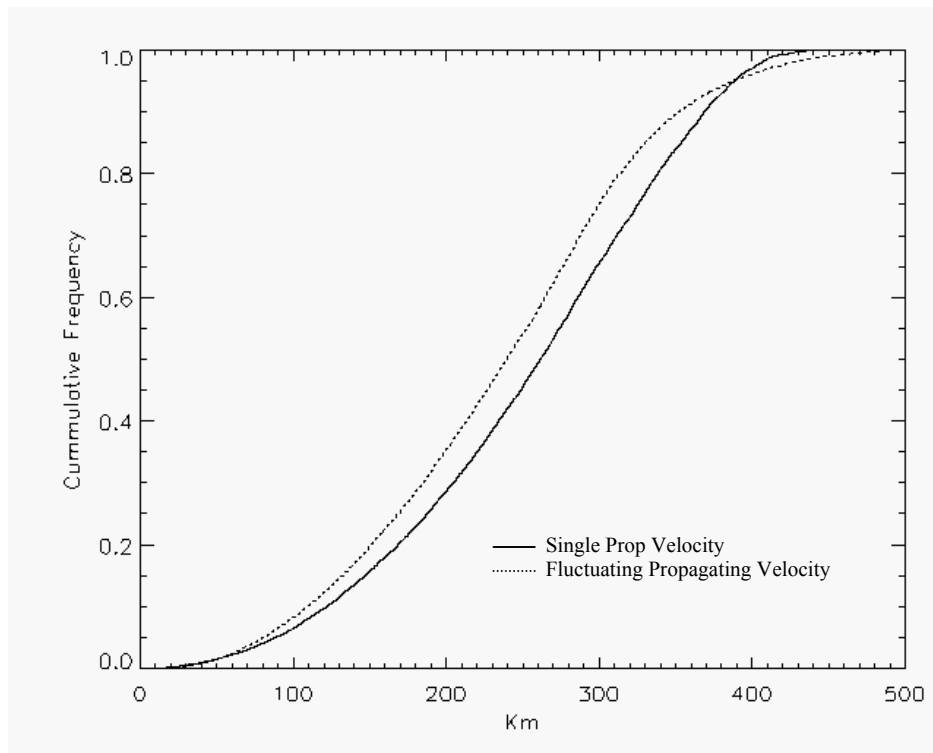


**Figure 7:** Cumulative frequencies of location retrieval errors determined over the U.S. East Coast based on a modeled sferics wave velocity versus a fixed (speed of light) velocity assumption.

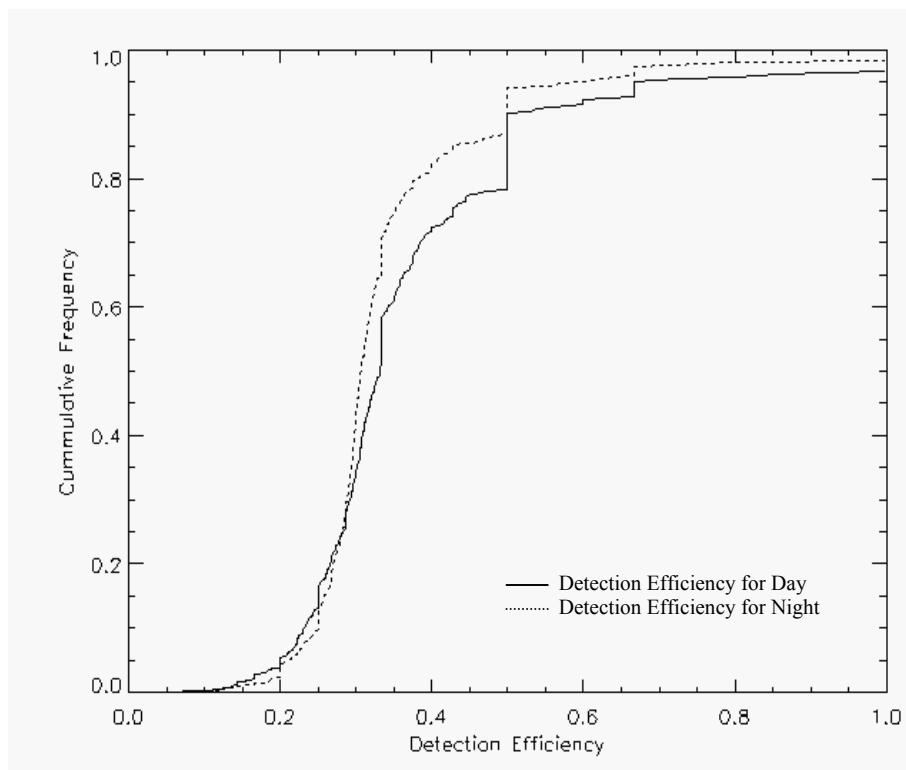


**Figure 8:** Cumulative frequency of Zeus's detection efficiency over the U.S. East Coast area for day (solid) and night (dotted) cases.